

Article citation info:

Guan Q, Zhang H, Jia L, Two-stage Remaining Useful Life Prediction Based on the Wiener Process With Multi-feature Fusion and Stage Division, *Eksploracja i Niezawodność – Maintenance and Reliability* 2024; 26(4) <http://doi.org/10.17531/ein/189803>

Two-stage Remaining Useful Life Prediction Based on the Wiener Process With Multi-feature Fusion and Stage Division

Indexed by:



Qingluan Guan^a, Zhongyi Zuo^{a,*}, Yanqin Teng^b, Huixian Zhang^c, Limin Jia^{c,d}

^a School of Traffic and Transportation Engineering, Dalian Jiaotong University, Dalian 116028, China

^b Qingdao Metro Group Corporation LTD, Qingdao 266035, China

^c School of Traffic and Transportation, Beijing Jiaotong University, Beijing 100044, China

^d State Key Laboratory of Advanced Rail Autonomous Operation, Beijing Jiaotong University, Beijing, 100044, China

Highlights

- A two-stage RUL prediction method based on the Wiener Process with multi-feature fusion and stage division is proposed.
- A linear feature fusion method is introduced for the CHI construction.
- A Z-score outlier detection strategy is introduced to address the issue of stage division in the degradation modeling.
- The proposed method is explained and the feasibility is proved by three analysis results of bearings.

Abstract

Remaining life prediction (RUL) is a critical link of maintenance decision-making, the accurate RUL prediction is an important means to monitor the operating status and achieve the safe operation of equipment. However, existing studies rarely considered the multi-stage characteristics of indicator fusion in the degradation process, and directly used the Wiener process to establish degradation model, which results in significant errors in RUL prediction results. Therefore, to solve above issues, a two-stage RUL prediction method based on the Wiener process model with multi-feature fusion and stage division is proposed in the paper. Firstly, the concept of multi-feature fusion is introduced to construct a comprehensive health indicator (CHI) that considers indicator performance. After that, a two-stage RUL prediction model based on the CHI is developed, and a method for detecting changing points and dividing stages is proposed. Finally, the effectiveness and predictability of the proposed method and CHI are demonstrated based on the bearing test datasets.

Keywords

remaining useful life, two-stage, multi-feature fusion, stage division, changing point

This is an open access article under the CC BY license (<https://creativecommons.org/licenses/by/4.0/>)

1. Introduction

Remaining useful life (RUL) plays a crucial role in the development of prognostics and health management (PHM), and the RUL prediction is the foundation and core of PHM. RUL prediction with the purpose of estimating the effective time interval from the current moment to failure [3,4]. In engineering, the accuracy of the RUL prediction has a significant impact on the safety, reliability, and maintenance costs of the equipment [5,6]. For example, the bearings are the key elements of rotating

machinery, such as, the aero-engine, bogie, and wind turbine units. If the failure probability can be accurately predicted in a period, it will help engineers detect the components that may fail in advance, perform timely maintenance or replacement, reduce maintenance costs, and ensure the safety operation of the equipment. RUL prediction methods are generally divided into the physical model-based method, data-driven method, and fusion method [7]. Data-driven RUL prediction plays a pivotal

(*) Corresponding author. Q. Guan (ORCID: 0000-0001-6320-4404) qlguan@bjtu.edu.cn, Z. Zuo (ORCID: 0000-0002-5229-0615) zuozy@bjtu.edu.cn, Y. Teng
E-mail addresses: 17120968@bjtu.edu.cn, H.Zhang.20114072@bjtu.edu.cn, L.Jia.0000-0003-2161-4637@bjtu.edu.cn, lmjia@bjtu.edu.cn,

role in the maintenance of the equipment. However, the individual health indicator (HI) cannot accurately describe the degradation process of the equipment, which leads to prediction errors. It is necessary to study the reasonable RUL prediction method to achieve the accurate prediction result.

HI is generally collected as the input for prognostics and predictive models, i.e. the condition monitoring and RUL prediction [8,9]. It contains the degradation information in the entire lifecycle of equipment. Most existing studies employed the individual performance indicator to depict the degradation characteristics. For example, the peak and kurtosis of bearing vibration signals. In engineering, the equipment has complex operating conditions, such as temperature, speed, and variable operating loads. Therefore, it is difficult to precisely describe the multi-variate degradation processes. It can lead to the issue of inaccurate RUL prediction due to ignoring the influence of other performance indicators. The study considering data fusion is designed to fuse multiple performance indicators (MPI) into a comprehensive health indicator (CHI). The main advantage of CHI is that it can comprehensively assess the current degradation state of the equipment, and it aims to improve the accuracy of RUL prediction [10].

Currently, there are two widely used HI: physical HI and virtual HI [11]. Physical HI is extracted through the simple analysis and processing of the original signals. For example, the existing literature commonly used individual time-domain feature to describe the degradation state of bearings, such as the average root mean square [12], root mean square [13], and peak [14]. Virtual HI is usually constructed by dimensionality reduction techniques and MPI fusion [15]. For instance, Widodo et al. [16] used principal component analysis (PCA) to perform the dimensionality reduction, further calculated the deviation between the unknown state and health state, which is used as CHI. Similarly, Liu et al. [17] employed PCA to reduce the dimension of the multiple features and constructed the CHI. Furthermore, Benkedjouh et al. [18] put forward a combination method of PCA and established isometric feature mapping for virtual HI construction.

In the existing studies, the data-driven RUL prediction method based on the one-dimensional degradation data has received considerable attention, whose data originates from the MPI fusion. For example, Liu et al. [19] made use of HI

functions to describe the link between HI and signal features for the CHI construction. Besides, a reliability prediction method based on artificial neural network support was proposed to realize the RUL prediction. In the statistical data-driven RUL prediction method, Aye and Heyns [20] proposed a fused Gaussian process regression method by studying the signals of low-speed bearings, and the result showed that it has good performance in RUL prediction with time-varying operating conditions. Song and Liu [21] utilized quantile regression to calculate the optimal fusion coefficient and constructed a data fusion model, which elevated the performance of RUL prediction. Li et al. [22] developed a novel nonlinear multi-feature method with the consideration of monotonicity, which improved the predictability in RUL prediction. Furthermore, Liu et al. [23] introduced the particle filtering to fuse the multi-sensor signals and achieved RUL prediction. Wu et al. [24] reformed the distributed Kalman filtering algorithm and completed RUL prediction with the fusion of the monitoring information. Chen et al. [25] completed HI construction by the feature fusion and constrained optimization, and accomplished the online RUL prediction based on the Wiener process. Liu et al. [26] fused the temperature data by PCA for CHI construction, and the RUL prediction based on the nonlinear Wiener model was carried out.

Even though the data-driven RUL prediction method based on the multi-feature fusion has achieved some good results, such as reduction of redundant information and improvement of prediction accuracy. However, there are several questions of the RUL prediction based on the multi-feature fusion still remain. On the one hand, some studies directly use multi-feature fusion methods to construct CHI, and rarely consider the impact of indicator performance such as the monotonicity (Mon), correlation (Corr), and robustness (Rob) on the prediction results. On the other hand, the existing studies rarely considered the multi-stage characteristics of fusion indicators during the degradation process, which leads to prediction biases in the single stage prediction, thereby effect the accuracy of RUL prediction.

In this paper, a two-stage RUL prediction method based on the Wiener Process with multi-feature fusion and stage division is proposed to solve the above-mentioned issues. The main contributions of the thesis are concluded as follows: (1) A linear

feature fusion method is introduced for the CHI construction. The various time-domain features that contain degradation information are selected considering Mon, Corr, and Rob. The PCA is applied to fuse the selected features, and the CHI is constructed to characterize the degradation process. (2) A Z-score outlier detection strategy is proposed to address the issue of stage division in degradation modeling. Besides, the quantitative standards are set for the stage division. The degradation path model is employed to fit the actual degradation path, and it is used to validate the rationality of health state division. (3) A two-stage RUL prediction method based on CHI is proposed. The degradation states that characterized by the CHI are distinct because of the different degradation stages of the equipment. Therefore, a staged RUL prediction model based on the first predicting time or fault occurrence time is developed, which can accurately match the corresponding changing time of each stage. (4) Three analysis results of bearings are provided. The proposed method based on CHI is compared with the prediction results based on the individual HI, which explicates the effectiveness and applicability of the proposed method.

The calculation framework of the proposed method is illustrated in Figure 1. The rest of this paper is organized as follows: Section 2 presents the process of CHI construction and evaluation. The stage division method and RUL prediction method based on CHI are discussed in Section 3. Section 4 provides the case study to demonstrate the applicability and effectiveness of the proposed method. The conclusion and future work are summarized in Section 5.

Table 1 The formulas of TTFs

TTF	Formula	TTF	Formula
Mean	$x_{am} = \frac{1}{N} \sum_{k=1}^N x_k$	Absolute mean (AM)	$x_m = \frac{1}{N} \sum_{k=1}^N x_k $
Maximum (Max)	$x_{max} = \max(x_k)$	Minimum (Min)	$x_{min} = \min(x_k)$
Peak	$x_p = \max x_k $	Peak-Peak (PP)	$x_{pp} = \max(x_k) - \min(x_k)$
Root mean square (RMS)	$x_{rms} = \sqrt{\frac{1}{N} \sum_{k=1}^N x_k^2}$	Variance (Var)	$x_{var} = \frac{1}{N} \sum_{k=1}^N (x_k - x_{am})^2$
Standard deviation (SD)	$x_{sd} = \sqrt{\frac{1}{N-1} \sum_{k=1}^N (x_k - \bar{x})^2}$	Square mean root (SRM)	$x_{smr} = \left(\frac{1}{N} \sum_{k=1}^N \sqrt{ x_k } \right)^2$
Skewness (Sk)	$x_{sk} = \frac{\sum_{k=1}^N (x_k - x_{am})^3}{[(N-1)x_{sd}^3]}$	Kurtosis (Ku)	$x_{ku} = \frac{\sum_{k=1}^N (x_k - x_{am})^4}{[(N-1)x_{sd}^4]}$
Shape factor (SF)	$x_{sf} = x_{rms} / x_{am}$	Crest factor (CF)	$x_{cf} = x_p / x_{rms}$
Margin factor (MF)	$x_{mf} = x_p / x_{smr}$	Impulse factor (IF)	$x_{if} = x_p / x_{am}$

¹ N is the number of sample points.

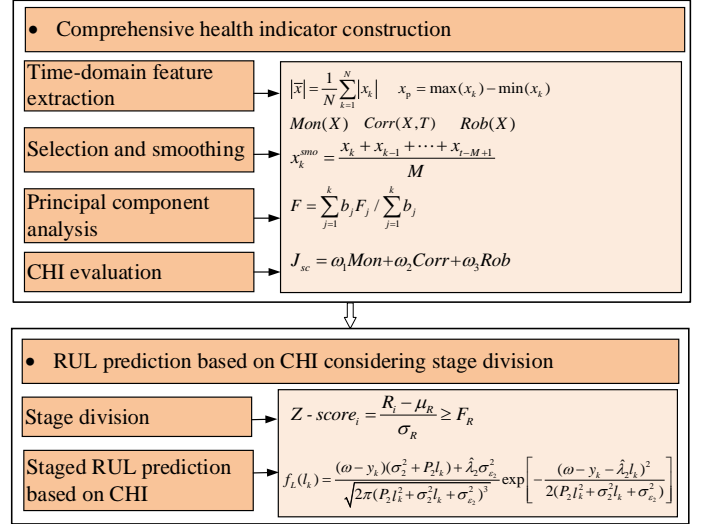


Fig. 1. Calculation framework of the proposed method.

2. Comprehensive health indicator construction

To overcome the shortcomings of CHI construction, it is necessary to consider the monotonicity (Mon), correlation (Corr), and robustness (Rob) of the performance indicators before degradation modeling. This section mainly introduces the CHI construction to achieve the above purpose. Firstly, the data preprocessing includes traditional time-domain feature (TTF) extraction, selection, and smoothing. After that, the MPI is linearly fused based on the PCA. The performance of the CHI is evaluated in the end.

2.1. Data preprocessing

Firstly, the TTF is extracted from the original vibration signals. The commonly used formulas of TTFs are given in Table 1.

Then, the appropriate TTF is selected to effectively depict the performance changes of the components in the entire lifecycle. The commonly used performance evaluation indicators mainly contain Mon, Corr and Rob [27-30]. To ensure the effectiveness of the selected TTF, the TTF should be removed if the Corr and Rob are less than 0.5 [31]. The feature goodness metrics of the Mon, Corr, and Rob are defined as follows

$$Mon(X) = |M_1 - M_2| / (n - 1) \quad (1)$$

$$Corr(X, T) = \frac{|\sum_{k=1}^n (x_k - \bar{X})(t_k - \bar{T})|}{\sqrt{\sum_{k=1}^n (x_k - \bar{X})^2 \sum_{k=1}^n (t_k - \bar{T})^2}} \quad (2)$$

$$Rob(X) = \frac{1}{n} \sum_{k=1}^n \exp\left(-\left|\frac{x_k - x_k^{smo}}{x_k}\right|\right) \quad (3)$$

where $X = [x_1, x_2, \dots, x_n]$ is the feature sequences of the entire life cycle. x_k represents the HI at time t_k . n is the total number of HI values. M_1 and M_2 is the number of positive and negative deviations, respectively. \bar{X} is the mean of HI values. \bar{T} is the mean of all operating cycles. x_k^{smo} is the average trend of HI at time t_k , generally, it is calculated by smoothing methods.

Finally, the moving average filtering (MAF) method is used to smooth the selected TTF sequence. It is expressed by

$$x_k^{smo} = \frac{x_k + x_{k-1} + \dots + x_{k-M+1}}{M} \quad (4)$$

where M is the length of the sliding window in the MAF method.

2.2 Multi-feature fusion based on the PCA

The individual TTF just characterizes a certain aspect of the degradation for the component, and the impacts of other TTFs are usually neglected. Despite the TTFs with poor Corr and Rob are eliminated, some duplicate or useless information still exists and affects the subsequent RUL prediction. Therefore, for the objective of applying the multivariate indicators to RUL prediction, a dimensionality reduction method is introduced to construct the CHI that can comprehensively describe the health status of equipment, which takes into account the Mon, Corr, and Rob of the indicators.

The CHI is constructed to provide a comprehensive and detailed description of the degradation state of the equipment. As one of the dimensionality reduction methods, the PCA method is a linear transformation for the original data sequence

[32]. It can not only reduce the dimensionality of multiple TTFs but also concentrate the advantages of each TTF. The flow chart of PCA is shown in Figure 2.

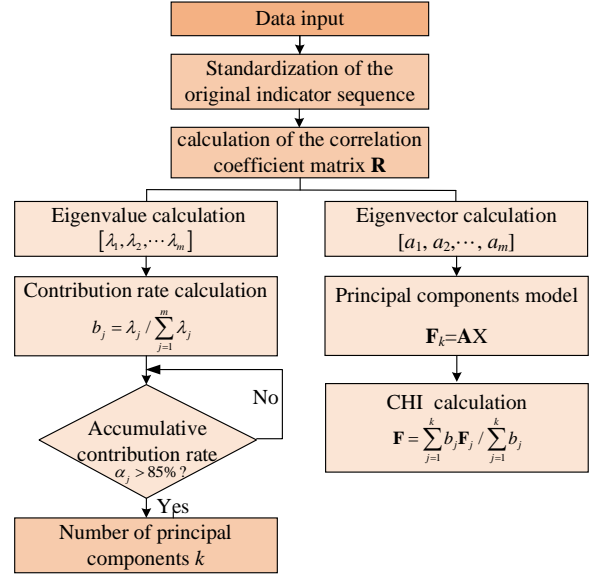


Fig. 2. The flow chart of PCA.

Firstly, the TTF sequence to be dimensionally reduced is constructed as an $n \times m$ matrix, and it is denoted as \mathbf{X} . It is represented as

$$\mathbf{X} = \begin{bmatrix} x_{11} & x_{12} & \dots & x_{1m} \\ x_{21} & x_{22} & \dots & x_{2m} \\ \vdots & \vdots & \vdots & \vdots \\ x_{n1} & x_{n2} & \dots & x_{nm} \end{bmatrix} \quad (5)$$

The main content of PCA includes standardization of the original indicator sequence, calculation of the correlation coefficient matrix, calculation of the eigenvalue and corresponding eigenvector, computation of the contribution rate and accumulative contribution rate in each component, and computation of the CHI.

Through the above steps, the principal component score is obtained by substituting each feature indicator sequence into the principal component expression. The calculation formula of k principal component models is given as

$$\begin{cases} \mathbf{F}_1 = a_{11}x_1 + a_{12}x_2 + \dots + a_{1m}x_m \\ \mathbf{F}_2 = a_{21}x_1 + a_{22}x_2 + \dots + a_{2m}x_m \\ \vdots \\ \mathbf{F}_k = a_{k1}x_1 + a_{k2}x_2 + \dots + a_{km}x_m \end{cases} \quad (6)$$

where $[a_1, a_2, \dots, a_m]$ is the unit eigenvector of the correlation coefficient matrix.

Finally, the fusion indicator \mathbf{F} is achieved by PCA, which is namely CHI. It is represented by

$$\mathbf{F} = \sum_{j=1}^k b_j \mathbf{F}_j / \sum_{j=1}^k b_j \quad (7)$$

where b_i is the contribution rate.

2.3. CHI evaluation

It is necessary to evaluate the performance of the CHI to verify its superiority. The individual evaluation indicator just describes part characteristics of the HI, which results in deviations or errors. Therefore, three performance evaluation indicators, that is, Mon, Corr, and Rob need to be considered comprehensively for the CHI evaluation. A weighted linear combination of the above metrics as the CHI evaluation criteria is introduced. The definition of the comprehensive evaluation metric (CEM) is given by

$$J_{sc} = \omega_1 Mon + \omega_2 Corr + \omega_3 Rob \quad (8)$$

$$s. t. \begin{cases} \omega_i > 0 \\ \sum_{i=1}^3 \omega_i = 1, i = 1,2,3 \end{cases}$$

where J_{sc} is the comprehensive evaluation indicator, ω_i is the weight of the individual metric.

The overall degradation trend of the equipment is required to be focused for RUL prediction, and the performance indicator should be provided with the monotonic trend. Thus, the weight of the Mon ought to be greater [27,28,31]. Take comprehensive consideration of different weights and the related reference [27], the weight of Mon, Corr, and Rob is set as 0.4, 0.3, and 0.3, respectively.

It can be observed that the CEM is both linearly and positively correlated with the individual metric. Furthermore, its value is limited to the range of [0, 1]. Therefore, it is also positively correlated with the predictive performance of CHI. It implies that the higher the CEM the RUL estimation is more effective. In addition, the CEM of the selected TTF should be higher for RUL prediction. The CEM can also be employed to prove the validity of feature selection.

3. RUL prediction based on CHI considering stage division

There are few studies introduced the CHI into the stage division, which ignored the impact of MPI on the degradation process and prediction results. It can improve the accuracy and reliability of RUL prediction by dividing the stages of CHI. The section

mainly introduces how to divide stages and predict RUL based on CHI to achieve the above objectives. The stage division is discussed first. Then, the staged RUL prediction method based on CHI is introduced.

3.1. Stage division

In practice, generally, the equipment will not suddenly transit from a normal state to failure. Therefore, it is more realistic to divide the degradation state into multiple stages for the equipment. The predictive model that conforms to the degradation trend is built for different stages of components.

To provide a more explicit description of the degradation process, the degradation state is divided into the health stage, minor damage stage, severe damage stage, and failure stage. The four stages correspond to three changing time, which are defined as the first predicting time (FPT), fault occurrence time (FOT), and failure time (FT). The schematic diagram of stage division is given in Figure 3.

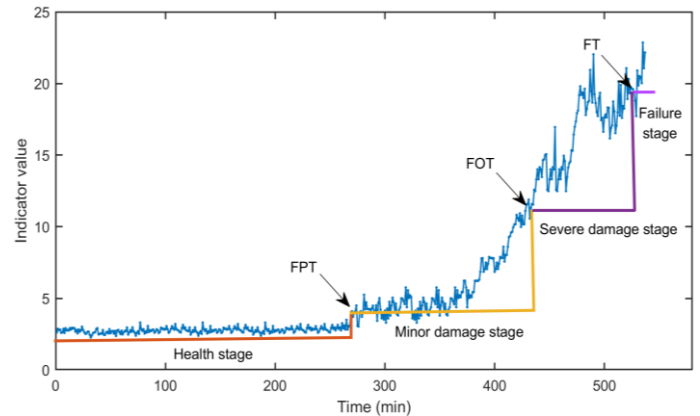


Fig. 3. The schematic diagram of stage division.

From Figure 3, the degradation state is divided into four stages. Health stage: the performance indicators of the equipment remain in the optimal state. Minor damage stage: the status of the equipment begins to degenerate as operating time increases, and the degradation state of the stage is not severe. It still is functioning normally. Severe damage stage: the equipment begins to accelerate degradation with continuous operation. The fault warning is supposed to be provided in the stage. Failure stage: the equipment steps into further deterioration and operates extremely unstable. The failure will occur if the the equipment continues to run, and the failure alarm should be informed.

The Z-score method is employed to resolve the issue of outlier detection. It can classify the degradation state exactly.

Shakya et al. [33] developed a novel methodology for online detection of degradation state. The paper is distinct from the above method, it divides degradation state by detecting the amplitude of CHI changes (i.e., degradation rate). Furthermore, in engineering, the degradation degree of the equipment is more intuitively characterized by the amplitude changes.

F_R is denoted as quantification criteria for the degradation state division. Firstly, F_R of each stage in the entire lifecycle is determined by sample data. Then, the Z-score method is utilized to detect the amplitude of CHI changes. $Z\text{-score}_i$ is the standard score. It is defined as

$$Z\text{-score}_i = \frac{R_i - \mu_R}{\sigma_R} \geq F_R \quad (9)$$

where R_i is the degradation rate at time t_i , which is calculated by taking the first-order derivative of the CHI. μ_R is the mean of degradation rate. σ_R is the standard deviation of the degradation rate.

In addition, for the verification of the rationality and applicability in stage division, the degradation path model is introduced to fit the degradation trajectories at each stage. The degradation process of the equipment is described using the deterministic function, which is represented by

$$Y(t) = f(t; \eta, \lambda) \quad (10)$$

where $f(t; \eta, \lambda)$ is the function of time. η is the deterministic parameter vector. λ is the random vector.

3.2. Two-staged RUL prediction modeling based on CHI

The construction, evaluation, and stage division of the CHI have been discussed. The CHI of the equipment is effectively divided into four stages through the above steps. It provides a good foundation for establishing an accurate degradation model. In the subsection, the staged RUL prediction based on CHI is introduced.

It is necessary to solve the issue of changing time detection to achieve the staged RUL prediction. The proposed method is different from Guan's method [34]. The changing time detection is transformed into the issue of stage division, which realizes accurate matching of the corresponding changing time in each stage. The FPT, FOT, and FT are acquired once the health stages of the equipment are divided. The FPT and FOT are utilized as the corresponding changing time of each stage in RUL

prediction, and then the RUL prediction based on the Wiener process is carried out.

Firstly, the health monitoring data represented by the CHI is denoted as Y . Let $Y(t)$ represent the degradation process of the equipment. The two-stage degradation model based on the Wiener process with measurement errors can be represented as

$$Y(t) = \begin{cases} y_0 + \lambda_1 t + \sigma_1 B(t) + \varepsilon_1, & t \leq \tau \\ y_\tau + \lambda_2(t - \tau) + \sigma_2 B(t - \tau) + \varepsilon_2, & t > \tau \end{cases} \quad (11)$$

where y_0 and y_τ are the initial states of the first and second stages, respectively. λ_1 , σ_1 and ε_1 are the drift coefficient, diffusion coefficient, and measurement error of the first stage, respectively. $B(t)$ is the standard Wiener process. τ is the changing time (the time of the changing point). λ_2 , σ_2 and ε_2 are the drift coefficient, diffusion coefficient, and measurement error of the second stage, respectively. It is generally assumed that the measurement errors of two stages are ε_1 and ε_2 , $\varepsilon_1 \sim N(0, \sigma_{\varepsilon_1}^2)$ and $\varepsilon_2 \sim N(0, \sigma_{\varepsilon_2}^2)$. It is worth noting that if the monitoring data is log linearized before degradation modeling, the model in equation (11) is consistent with Guan's model [34].

After that, the first hitting time (FHT) [35] is introduced to define the lifetime of the equipment. It is defined by

$$T = \inf\{t: Y(t) \geq \omega | Y(0) \leq \omega\} \quad (12)$$

where ω is the failure threshold. $Y(t_k)$ is the observations at the current time t_k , $y_k = Y(t_k)$. The RUL at time t_k is defined based on the FHT $L = \inf\{l: Y(t_k + l) \geq \omega | Y(t_k) \leq \omega\}$.

Considering the randomness of the degradation state at changing time and the random model parameters, if $\lambda_1 \sim N(\hat{\lambda}_1, P_1)$, $\lambda_2 \sim N(\hat{\lambda}_2, P_2)$, the probability density function (PDF) of the two-stage RUL at time t_k are as follows

Case 1: The current time t_k is less than τ , then the PDF of RUL is given by

$$f_L(l_k) = \begin{cases} \frac{(\omega - y_k)(\sigma_1^2 + P_1 l_k) + P_1 \tau^2 \hat{\lambda}_1}{\sqrt{2\pi(P_1 l_k^2 + \sigma_1^2 l_k + P_1 \tau^2)^3}} \exp\left[-\frac{(\omega - y_k - \hat{\lambda}_1 l_k)^2}{2(P_1 l_k^2 + \sigma_1^2 l_k + P_1 \tau^2)}\right], & l + t_k \leq \tau \\ A - B, & l + t_k > \tau \end{cases} \quad (13)$$

where

$$A = \frac{P_2 l_k + \sigma_2^2}{\sqrt{2\pi P_a^2 (P_a + P_b)}} \exp\left[-\frac{(a - b)^2}{2(P_a + P_b)}\right] \\ \times \left\{ \frac{bP_a + aP_b}{P_a + P_b} \Phi\left(\frac{bP_a + aP_b}{\sqrt{P_a P_b (P_a + P_b)}}\right) + \frac{\sqrt{P_a P_b}}{\sqrt{P_a + P_b}} \Phi\left(\frac{bP_a + aP_b}{\sqrt{P_a P_b (P_a + P_b)}}\right) \right\} \\ + \frac{\hat{\lambda}_2 \sigma_2^2}{\sqrt{2\pi P_a^2 (P_a + P_b)}} \exp\left[-\frac{(a - b)^2}{2(P_a + P_b)}\right] \left\{ 1 - \Phi\left(-\frac{bP_a + aP_b}{\sqrt{P_a P_b (P_a + P_b)}}\right) \right\}$$

$$B = \frac{P_2 l_k + \sigma_2^2}{\sqrt{2\pi P_a^2(P_a + P_b)}} \exp \left[\frac{2\hat{\lambda}_1(\omega - y_k)(\tau - t_k)}{\sigma_1^2(\tau - t_k) + \sigma_{\varepsilon_1}^2} + \frac{2(\omega - y_k)^2 P_1 \tau^2}{(\sigma_1^2(\tau - t_k) + \sigma_{\varepsilon_1}^2)^2} \right]$$

$$\times \exp \left[-\frac{(a - c)^2}{2(P_a + P_b)} \right]$$

$$\times \left\{ \frac{cP_a + aP_b}{P_a + P_b} \phi \left(\frac{cP_a + aP_b}{\sqrt{P_a P_b(P_a + P_b)}} \right) + \frac{\sqrt{P_a P_b}}{\sqrt{P_a + P_b}} \phi \left(\frac{cP_a + aP_b}{\sqrt{P_a P_b(P_a + P_b)}} \right) \right\}$$

$$+ \frac{\hat{\lambda}_2 \sigma_{\varepsilon_2}^2}{\sqrt{2\pi P_a^2(P_a + P_b)}} \exp \left[\frac{2\hat{\lambda}_1(\omega - y_k)(\tau - t_k)}{\sigma_1^2(\tau - t_k) + \sigma_{\varepsilon_1}^2} + \frac{2(\omega - y_k)^2 P_1 \tau^2}{(\sigma_1^2(\tau - t_k) + \sigma_{\varepsilon_1}^2)^2} \right]$$

$$\times \exp \left[-\frac{(a - c)^2}{2(P_a + P_b)} \right] \left\{ 1 - \Phi \left(-\frac{bP_a + aP_b}{\sqrt{P_a P_b(P_a + P_b)}} \right) \right\}$$

$$a = \hat{\lambda}_2(l_k - \tau + t_k), b = \omega - y_k - \hat{\lambda}_1(\tau - t_k),$$

$$c = -\omega + y_k - \hat{\lambda}_1(\tau - t_k) - P_1(\tau - t_k)^2 / [\sigma_1^2(\tau - t_k) + \sigma_{\varepsilon_1}^2],$$

$$P_a = P_2(l_k - \tau + t_k)^2 + \sigma_2^2(l_k - \tau + t_k) + \sigma_{\varepsilon_2}^2,$$

$$P_b = P_1(\tau - t_k)^2 + \sigma_1^2(\tau - t_k) + \sigma_{\varepsilon_1}^2.$$

Case 2: The current time t_k is greater than τ , then the PDF of RUL is given by

$$f_L(l_k) = \frac{(\omega - y_k)(\sigma_2^2 + P_2 l_k) + \hat{\lambda}_2 \sigma_{\varepsilon_2}^2}{\sqrt{2\pi(P_2 l_k^2 + \sigma_2^2 l_k + \sigma_{\varepsilon_2}^2)^3}} \exp \left[-\frac{(\omega - y_k - \hat{\lambda}_2 l_k)^2}{2(P_2 l_k^2 + \sigma_2^2 l_k + \sigma_{\varepsilon_2}^2)} \right] \quad (14)$$

Finally, the estimated RUL is computed through the definition of mathematical expectation, and the model parameters are updated and estimated by the expectation maximization (EM) algorithm [34,36].

4. Case study

In this section, the case study is conducted by the XJTU-SY bearing datasets [37]. To verify the predictability and superiority of CHI in RUL prediction, the proposed method is compared with Guan's method [34] and Si's method [38]. The degradation data of the bearing has an exponential trend. For the fair comparison, the data need to be log-linearized in degradation modeling. Furthermore, the RUL prediction based on CHI and peak is conducted, respectively.

4.1. Data description

The XJTU-SY bearing datasets have been widely used in the study of data-driven RUL prediction because of the complete entire lifecycle data and good mathematical characteristics. The peak is selected as the individual indicator owing to its changing character is evident and profit for calculation.

Firstly, the vibration signal of the bearing is preprocessed. Then, the CHI is constructed based on the selected multivariate TTFs, and the health state is divided. Finally, the RUL prediction

based on CHI is conducted and the prediction results are compared with the results based on the peak. The selected samples are shown in Table 2.

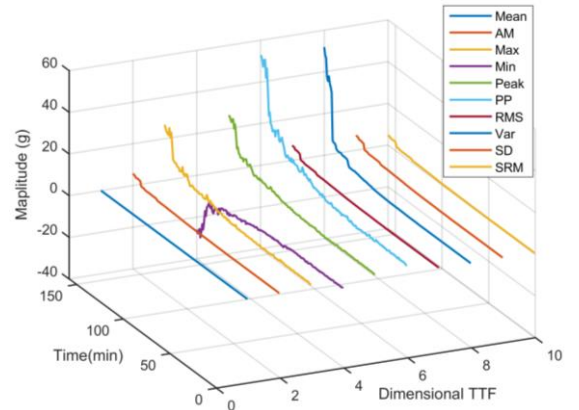
Table 2. The selected samples.

Datasets	Actual RUL (min)	Time interval (min)
Bearing 1_1	123	1
Bearing 1_3	158	1
Bearing 2_5	339	1

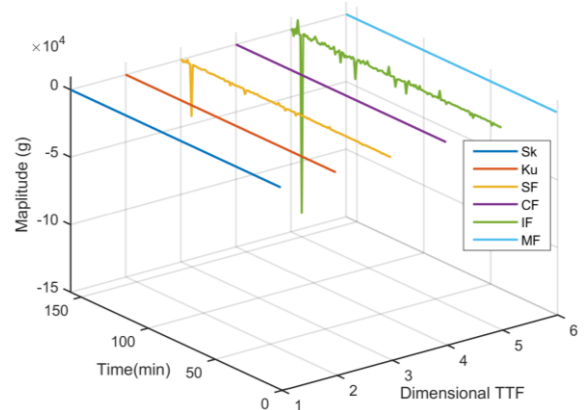
4.2. RUL prediction of Bearing 1_3

4.2.1. Extraction and selection

The TTFs of Bearing1_3 are selected based on Mon, Corr, and Rob. Sixteen TTFs of the bearing are extracted, and the extracted TTFs are displayed in Figure 4.



(a) The dimensional TTF values



(b) The dimensionless TTF values

Fig. 4. The extracted TTF.

The evaluation results of the above sixteen TTFs are presented in Figure 5. As shown in Figure 5, the Mon of each TTF is not high. The Corr and Rob of the TTFs are less than 0.5 which are difficult for RUL prediction effectively and efficiently. Therefore, nine TTFs, including AM, Max, Min, Peak, PP, RMS, Var, SD, and SRM are selected as the multivariate performance

indicators for CHI construction. Furthermore, the MAF method is applied for smoothing.

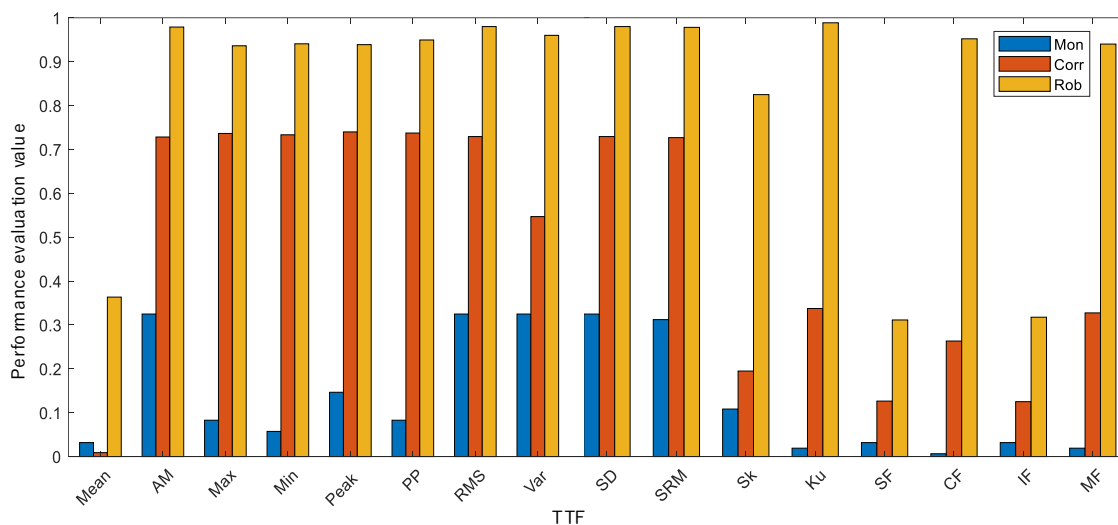


Fig. 5. The performance evaluation results of the TTF.

4.2.2. CHI construction and evaluation

Next, PCA is employed to process the selected TTFs. There are 158 observations in every TTF, and the TTF sequence of Bearing 1_3 is 158×9 th order matrix. The CHI of the sample is $F=F_1$. The CHI of Bearing 1_3 is given in Figure 6.

The evaluation results of the CHI are compared with the original nine TTFs. The comparison results of indicators are given in Table 3. From the Table 3, it is very apparent that the Mon, Corr, Rob, and the CEM of CHI are superior to the individual TTFs. Therefore, the applicability and validity of CHI are better than the individual indicators.

Table 3. The comparison results of indicators.

Indicator	Mon	Corr	Rob	CEM	Indicator	Mon	Corr	Rob	CEM
AM	0.3248	0.7283	0.9789	0.6421	RMS	0.3248	0.7293	0.9800	0.6427
Max	0.0828	0.7364	0.9362	0.5349	Var	0.3248	0.5469	0.9600	0.5820
Min	0.0573	0.7333	0.9407	0.5251	SD	0.3248	0.7293	0.9800	0.6427
Peak	0.1465	0.7399	0.9388	0.5622	SRM	0.3121	0.7269	0.9782	0.6364
PP	0.0828	0.7373	0.9494	0.5391	CHI	0.4650	0.7105	0.9844	0.6945

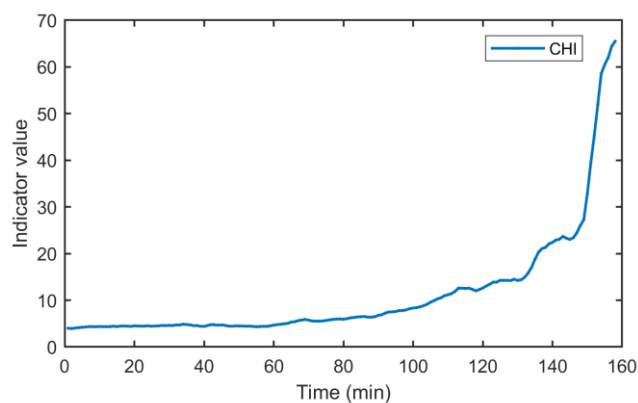


Fig. 6. The CHI of Bearing 1_3

4.2.3. Stage division and validation

It is assumed that the corresponding quantification criteria of each stage are 0.5, 1, and 3, respectively. The outlier detection is performed based on Equation (9) and CHI. The degradation state of the sample is divided into four stages: health stage ($|Z$ -

score $|\leq 0.5$), minor damage stage ($0.5 < |Z$ -score $|\leq 1$), severe damage stage ($1 < |Z$ -score $|\leq 3$), and failure stage ($|Z$ -score > 3). The outlier detection result of the Z-score method is visualized in Figure 7.

From Figure 7, it can be observed that there are several outlier

detection points in each stage. The first anomaly occurrence time is defined as the initial time of the stage. The FPT $\tau_1 = 112\text{min}$, FOT $\tau_2 = 134\text{min}$, and FT $\tau_3 = 149\text{min}$.

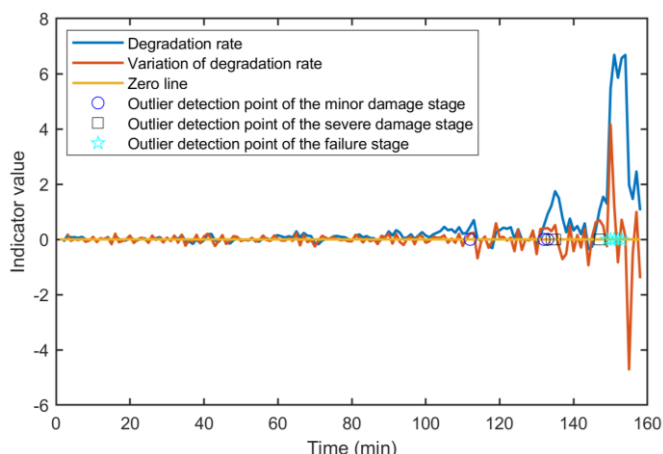


Fig. 7. The outlier detection result of Z-score method.

The stage division result of the sample is shown in Figure 8. It depicts that the degradation state of the sample is divided into four stages. Health stage: $0 < |Z\text{-score}| \leq 0.5$. The degradation rate of bearing is in the normal range. The fluctuation of the degradation rate tends to zero, which indicates that it is a constant. Minor damage stage: $0.5 < |Z\text{-score}| \leq 1$. The degradation rate is without abnormal values. However, the degradation rate begins to suffer from fluctuations, which are caused by the abnormal vibrations. Severe damage stage: $1 < |Z\text{-score}| \leq 3$. The degradation rate exists in abnormal values. The fluctuation of the degradation rate becomes larger and more evident with time increasing. Further, the bearing starts to accelerate the degeneration. Failure stage: $|Z\text{-score}| > 3$. The degradation rate has a high degree of abnormal values. Most fluctuations in the degradation rate are very large and obvious. The failure occurs in the stage.

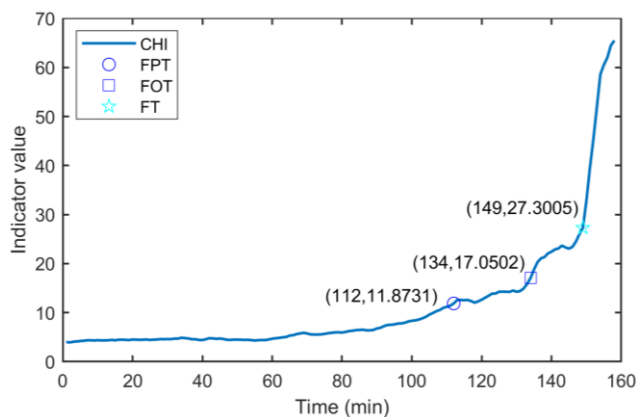


Fig. 8. The stage division result of Bearing 1_3.

The commonly used single exponential function is applied

to describe the degradation process of bearing, which is employed to verify the rationality of the stage division. The exponential degradation model is described by

$$Y(t) = a \exp(bt) + c \quad (15)$$

where a , b , and c are the coefficients, which are estimated by the least squares method.

The fitted degradation path after time t_k is calculated by Equation (15). The fitting results of the degradation path in each stage are demonstrated in Figure 9.

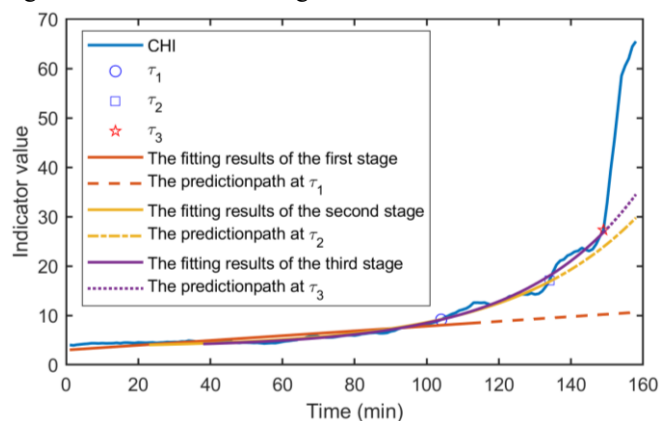


Fig. 9 The fitting results of the degradation path in each stage.

As shown in Figure 9, the fitting result of the CHI is $y_1 = 0.04837t + 2.985$ in the first stage. The degradation rate is approximately 0.04837. The stage is the health stage and consistent with the stage division results. The fitting result of the second stage is $y_2 = 0.3098e^{0.02812t} + 3.429$. The prediction deviation at $\tau_1 = 112\text{min}$ is large, which indicates that the degradation rate has changed and the bearing enters the minor damage stage. The result is consistent with the stage division. In the third stage, the fitting result is $y_3 = 0.2082e^{0.03166t} + 3.534$. Compared with the prediction result at $\tau_2 = 134\text{min}$, the bearing begins to deteriorate, which indicates that the warning should be provided. It agrees with stage division result. The prediction result after $\tau_3 = 149\text{min}$ is extremely high. It indicates that the performance of the bearing is rapidly decreasing in the fourth stage. The stage has the risk of failure and the failure alarm is supposed to be notified, which is in accord with the stage division. The above results adequately explain that the proposed stage division method is reasonable and applicable.

4.2.4. RUL prediction and analysis

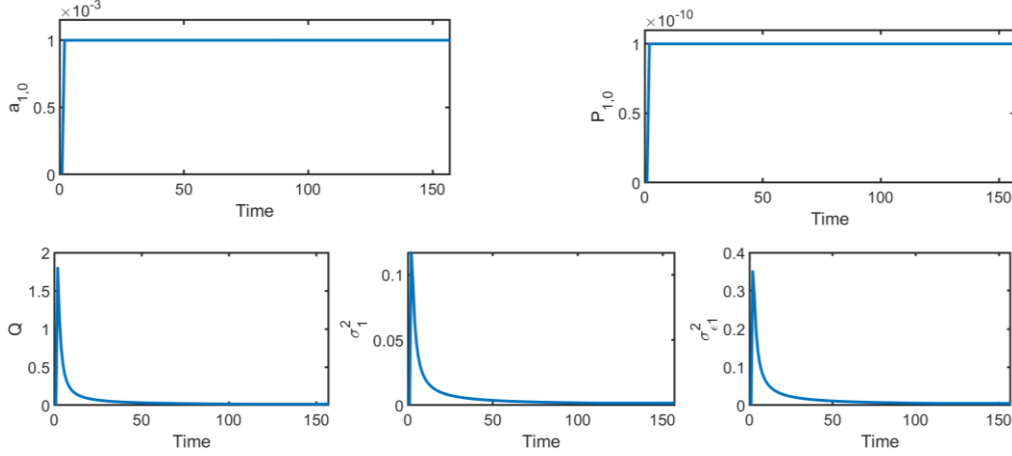
The failure threshold is set as 65.5 based on the degradation trend. $\tau_1 = 112\text{min}$ is defined as the changing time in the subsequent two-stage RUL prediction, which is set according to

the stage division results.

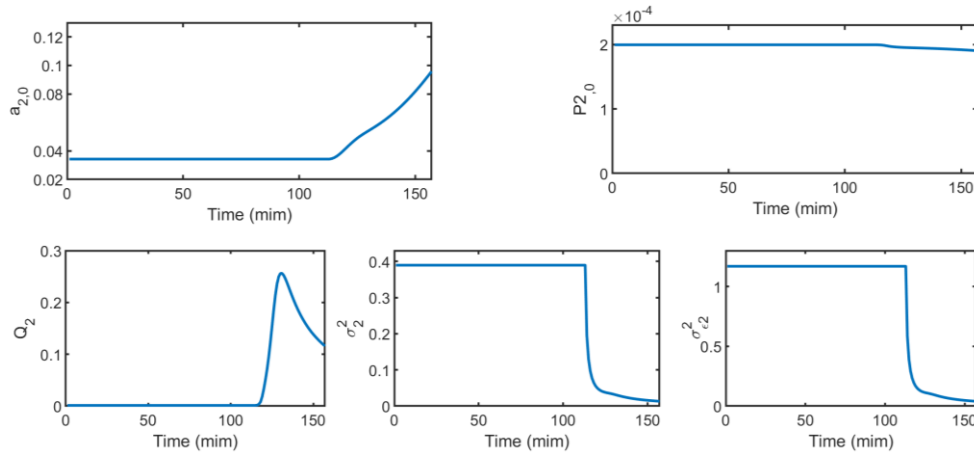
Furthermore, the model parameters of the two stages are represented by $\Theta_1 = [a_{1,0}, P_{1,0}, Q_1, \sigma_1^2, \sigma_{\varepsilon_1}^2]^T$ and $\Theta_2 = [a_{2,0}, P_{2,0}, Q_2, \sigma_2^2, \sigma_{\varepsilon_2}^2]^T$, respectively. Correspondingly, the initial values of the model parameters are set as $\Theta_1 =$

$[0.001, 1 \times 10^{-10}, 0.01, 1 \times 10^{-4}, 1 \times 10^{-4}]^T$ and $\Theta_2 = [0.031, 2 \times 10^{-4}, 0.001, 0.001, 0.15]^T$.

Considering the random model parameters, the EM algorithm is applied to estimate the model parameters. The estimation results of model parameter are shown in Figure 10.



(a) Parameter estimation of the first stage



(b) Parameter estimation of the second stage

Fig. 10. The estimation results of model parameter.

As shown in Figure 10, the model parameters of the two stages gradually converge with the accumulation of the monitoring time, which indicates the feasibility and stability of the proposed method. Furthermore, it can be seen that there are obvious differences in the drift coefficient, diffusion coefficient, and measurement error between the first and second stage. It further confirms that the degradation process characterized by the CHI has the two-stage characteristics, which is consistent with the hypothesis. Therefore, it is necessary and reasonable to conduct the two-stage degradation modeling for the degradation process.

According to the above estimation results, the PDF of RUL in each stage is calculated by the Equation (13) and Equation

(14). And then, the RUL prediction results is estimated by the definition of mathematical expectations, which are compare with the Guan's method [34]. In addition, the RUL prediction results based on CHI and peak are compared with each other for the verification of the CHI performance. The RUL prediction results at each monitoring time are given in Figure 11. As described in Figure 11, it is apparent that the RUL prediction based on CHI fits the actual RUL very well. For example, the actual RUL is 46min at the changing time $t=112$ min. The estimated RUL of the proposed method is 45.13min with relative error (RE) of 0.0189. The estimation result of Guan's method is 43.62min, and the RE is 0.0518. The prediction accuracy of the proposed method is improved by 3.29%. It

indicates that the better RUL prediction result is acquired by the CHI construction in degradation modeling, that is, considering the fusion of multi-feature fusion.

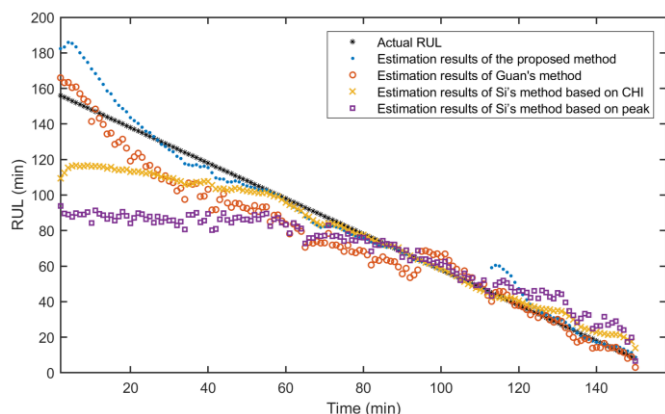


Fig. 11. The RUL prediction results at each monitoring time.

The RE is computed to intuitively describe the predictive performance of the proposed method. The RE at each monitoring time is visualized shown in Figure 12.

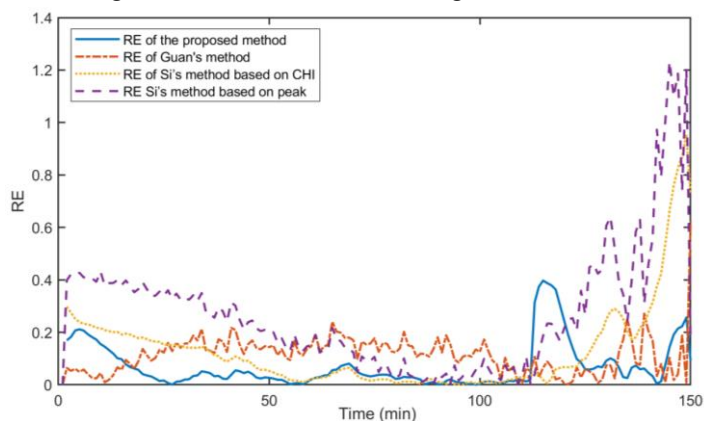


Fig. 12. The RE at each monitoring time.

Figure 12 reveals that the RE of the proposed method is below 0.08 in the monitoring intervals [18,58] and [133,143]. The average RE of Guan's method and Si's method based on peak are 0.1135 and 0.2665, respectively. The average RE of the proposed method and Si's method based on CHI are 0.0696 and 0.1298, respectively. Specifically, the average prediction accuracy of the proposed method and Si's method based on CHI are improved by 4.39% and 13.67%, respectively. It indicates that the accuracy of RUL prediction is significantly improved by integrating the CHI into the degradation modeling. The results are consistent with the showed results in Figure 11, which demonstrates that the proposed method can realize better

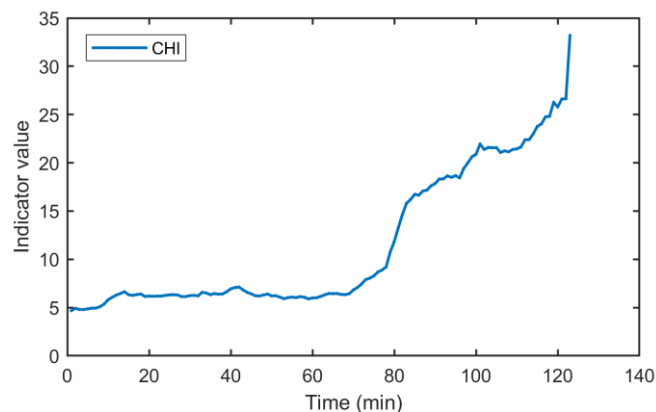
RUL prediction.

4.3. RUL prediction of other experimental data

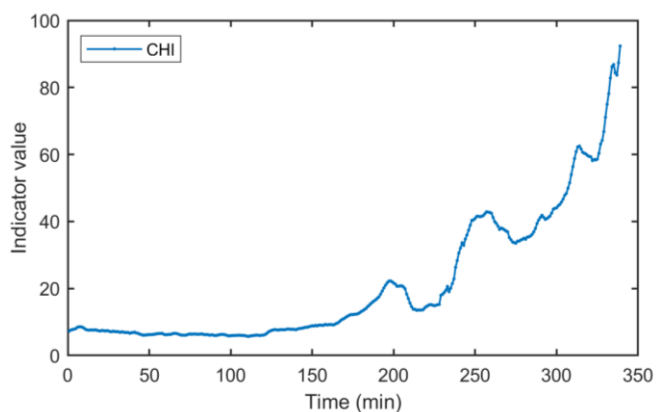
Further, to validate the applicability and superiority of the proposed method, the RUL prediction results of Bearing 1_1 and Bearing 2_5 are used for comparative study.

4.3.1. CHI construction and stage division

Firstly, the PCA is applied for the CHI construction. The CHI of Bearing 1_1 and Bearing 2_5 are given in Figure 13.



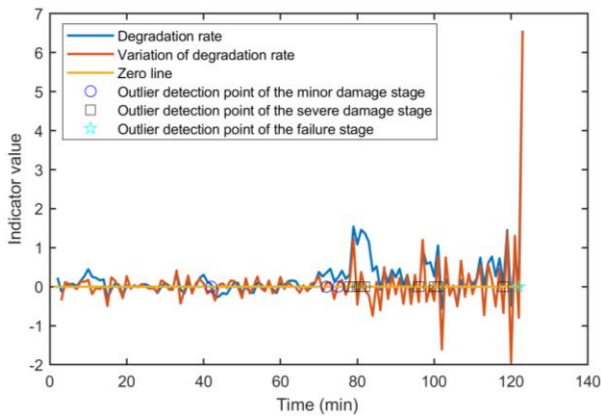
(a) The CHI of Bearing 1_1



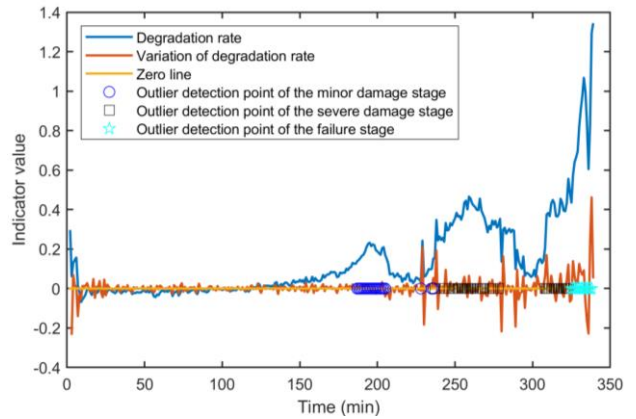
(b) The CHI of Bearing 2_5

Fig. 13. The CHI of Bearing 1_1 and Bearing 2_5

Then, the outlier detection results of the Z-score method for Bearing 1_1 and Bearing 2_5 are shown in Figure 14. Figure 14 reveals that the first outlier detection of each stage is taken as the initial time of the stage. The FPT, FOT, and FT of Bearing 1_1 are $\tau_1=42\text{min}$, $\tau_2=78\text{min}$, and $\tau_3=122\text{min}$, respectively. For Bearing 2_5, the FPT $\tau_1=187\text{min}$, FOT $\tau_2=237\text{min}$, and FT $\tau_3=325\text{min}$.



(a) The outlier detection result of Bearing 1_1

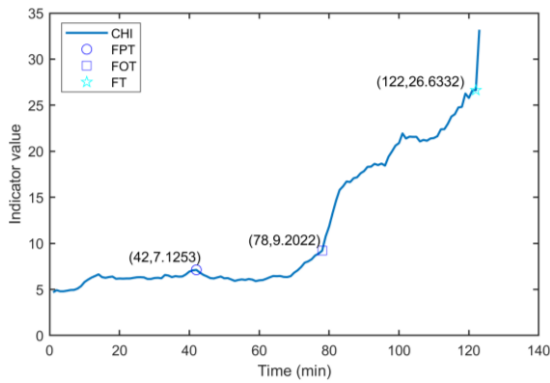


(b) The outlier detection result of Bearing 2_5

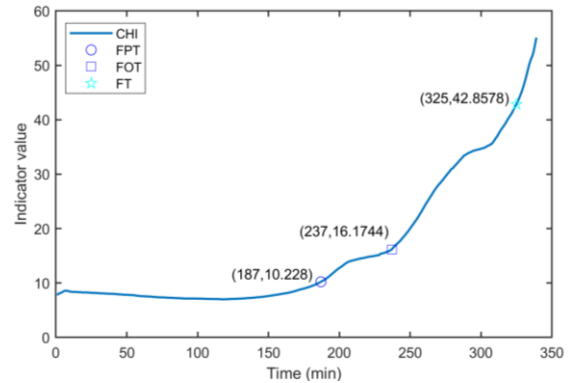
Fig. 14 The outlier detection result of Z-score method for Bearing 1_1 and Bearing 2_5.

The stage division results of the samples are given in Figure 15. It is cleared that the degradation state of Bearing1-3 and Bearing2-5 are divided into the health stage, minor damage stage, severe damage stage, and failure stage. The online

monitoring of the equipment should be strengthened in the severe damage stage and failure stage to avoid unnecessary losses.



(a) The classification results of Bearing 1_1



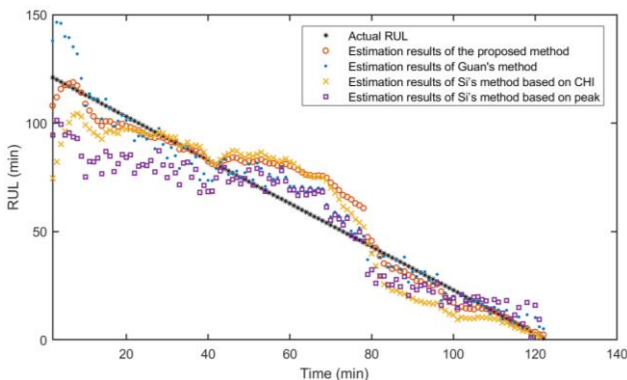
(b) The classification results of Bearing 2_5

Fig. 15. The stage division results of Bearing 1_1 and Bearing 2_5.

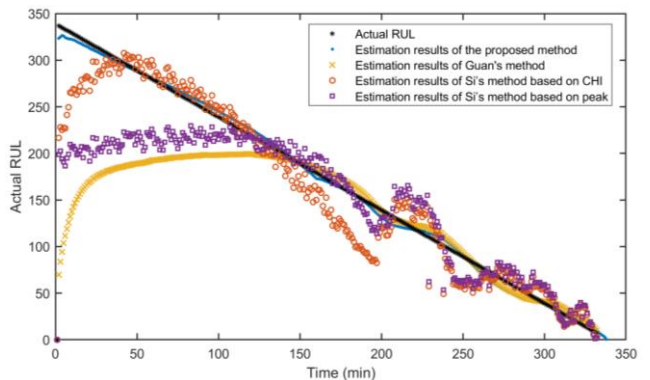
4.3.2. RUL prediction and comparison

The RUL prediction results based on CHI and peak are

conducted for comparison. The RUL prediction results of Bearing 1_1 and Bearing 2_5 are shown in Figure 16.



(a) The prediction results of Bearing 1_1



(b) The prediction results of Bearing 2_5

Fig. 16. The RUL prediction results of Bearing 1_1 and Bearing 2_5.

From Figure 16, it can be concluded that the RUL estimations of the proposed method are closer to the actual RUL than other methods. For instance, in Figure 16(a), the actual

RUL of Bearing 1_1 is 11min at time $t=112$ min. The RUL prediction of the proposed method is 10.70min with RE 0.0270, which indicates that the estimation results of the proposed

method match the actual RUL well. For Bearing 2_5, in Figure 16(b), the actual RUL is 119min at time $t=220$ min. The estimated RUL of the proposed method is 117.8 min and the corresponding RE is 0.0101. The estimation of Guan's method is 128.35min, and the RE is 0.0786. The results show that the RUL prediction of the proposed method is optimal, and the better RUL prediction results are achieved by considering the multi-feature fusion.

The RE of each method is calculated for the intuitive description of the predictive performance of the proposed method. Specifically, the average RE of each method is given in Table 4. The average RE of each method.

Quantitative indicators	Datasets	Si's method based on peak	Si's method based on CHI	Guan's method	The proposed method
Average RE	Bearing 1-3	0.2665	0.1298	0.1135	0.0696
	Bearing 1-1	0.3277	0.2176	0.1855	0.1391
	Bearing 2-5	0.2122	0.1777	0.1704	0.0636

5. Conclusions

A two-stage RUL prediction method with multi-feature fusion is proposed for the issue of MPI fusion. PCA is introduced to analyze the various degradation information of the equipment by linear fusion. The dimension reduction fusion is accomplished and the CHI is constructed. The comprehensive evaluation of the performance is conducted based on Mon, Corr, and Rob. Furthermore, the Z-score method is applied to solve the issue of identifying the changing time of each degradation stage, and the quantification criteria are set to achieve stage division. The degradation state is divided into the health stage, minor damage stage, severe damage stage, and failure stage. The degradation path model is used to fit the degradation path of each stage, which verifies the rationality and applicability of the stage division. A two-staged RUL prediction model based on

Table 4. In Table 4, the average RE of the proposed method is the minimum compared with the corresponding RUL prediction method based on peak. For Bearing 1_1, compared to Guan's method and Si's method based on peak, it should be noted that the average RE of the proposed method and Si's method based on CHI decreased by 4.64% and 11.01%, respectively. Similarly, the average RE of the RUL prediction based on CHI for Bearing 2_5 decreased by 10.68% and 3.45%, respectively. The case analysis results of the two samples further validate the applicability and superiority of RUL prediction based on the multi-feature fusion and stage division.

CHI is proposed. Finally, the comparative analysis is conducted on the RUL prediction based on CHI and peak by three samples of the XJTU-SY bearing datasets. The results indicate that the CHI has superiority in RUL prediction, and the proposed method contributes to improving the accuracy of RUL prediction.

However, despite the encouraging prediction results, there are still some issues that need further study. The linear correlation between the MPI is taken into consideration in degradation modeling. In practical engineering, for the equipment, the correlation relationship of the performance indicators is more complicated. Therefore, as a direction for future study, it is suggested to consider the complex nonlinear correlation of the MPI in RUL prediction. In addition, the multi-stage RUL prediction will be another direction worth studying in the future.

Acknowledgment

This research was funded by the Fundamental Research Funds for the Central Universities (Science and technology leading talent team project, Grant No.2022JBQY007).

Reference

- Vichare N M, Pecht M G. Prognostics and health management of electronic. *IEEE Transactions on Components and Packaging Technologies*, 2006, 29(1): 222-229, <https://doi.org/10.1109/TCAPT.2006.870387>.
- Camci F, Chinnam R B. Health-state estimation and prognostics in machining processes, *IEEE Transactions on Automation Science and Engineering*, 2010, 7(3): 581-583, <https://doi.org/10.1109/TASE.2009.2038170>.

3. Li K, Ren L, Li X, et al. Remaining useful life prediction of equipment considering dynamic thresholds under the influence of maintenance. *Eksploatacja i Niezawodność - Maintenance and Reliability*, 2024, 26(1): 174903, <https://doi.org/10.17531/ein/174903>.
4. Wang Z, Shangguan W, Peng C, et al. Similarity based remaining useful life prediction for lithium-ion battery under small sample situation based on data augmentation. *Eksploatacja i Niezawodność -Maintenance and Reliability*, 2024, 26(1): 175585, <https://doi.org/10.17531/ein/175585>.
5. Lei Y G, Li N P, Guo L, et al. Machinery health prognostics: A systematic review from data acquisition to RUL prediction, *Mechanical systems and signal processing*, 2018, 104: 799-834, <https://doi.org/10.1016/j.ymssp.2017.11.016>.
6. Zhang Z X, Si X S, Hu C H, et al. Degradation data analysis and remaining useful life estimation: A review on Wiener process-based methods, *European Journal of Operational Research*, 2018, 271(3): 775-796, <https://doi.org/10.1016/j.ejor.2018.02.033>.
7. Pecht M. *Prognostics and health management of electronics*, New Jersey: Wiley Online Library, 2008, <https://doi.org/10.1002/9780470385845>.
8. Cheng Y, Wu J, Zhu H, et al. Remaining useful life prognosis based on ensemble long short-term memory neural network, *IEEE Transactions on Instrumentation and Measurement*, 2020, 70: 1-12, <https://doi.org/10.1109/TIM.2020.3031113>.
9. Wu J, Hu K, Cheng Y, et al. Data-driven remaining useful life prediction via multiple sensor signals and deep long short-term memory neural network, *ISA transactions*, 2020, 97: 241-250, <https://doi.org/10.1016/j.isatra.2019.07.004>.
10. Chen J L, Jing H J, Chang Y H, et al. Gated recurrent unit based recurrent neural network for remaining useful life prediction of nonlinear deterioration process, *Reliability Engineering & System Safety*, 2019, 185: 372-382, <https://doi.org/10.1016/j.res.2019.01.006>.
11. Hu C, Youn B D, Wang P F, et al. Ensemble of data-driven prognostic algorithms for robust prediction of remaining useful life, *Reliability Engineering & System Safety*, 2012, 103: 120-135, <https://doi.org/10.1016/j.res.2012.03.008>.
12. Li P, Liu X, Yang Y. Remaining useful life prognostics of bearings based on a novel spatial graph-temporal convolution network. *Sensors (Basel)*, 2021, 21(12): 4217, <https://doi.org/10.3390/s21124217>.
13. Li Y X, Huang X Z, Ding P F, et al. Wiener-based remaining useful life prediction of rolling bearings using improved Kalman filtering and adaptive modification, *Measurement*, 2021, 182: 109706, <https://doi.org/10.1016/j.measurement.2021.109706>.
14. Liu M J, Dong Z S, Shi H, et al. Remaining useful life estimation of fan slewing bearings in nonlinear Wiener process with random covariate effect, *Shock and Vibration*, 2022, 2022: 1-19, <https://doi.org/10.1155/2022/5441760>.
15. Anowar F, Sadaoui S, Selim B. Conceptual and empirical comparison of dimensionality reduction algorithms (PCA, KPCA, LDA, MDS, SVD, LLE, ISOMAP, LE, ICA, t-SNE). *Computer Science Review*, 2021, 40: 100378, <https://doi.org/10.1016/j.cosrev.2021.100378>.
16. Widodo A, Yang B S. Application of relevance vector machine and survival probability to machine degradation assessment, *Expert Systems with Applications*, 2011, 38(3): 2592-2599, <https://doi.org/10.1016/j.eswa.2010.08.049>.
17. Liu Y C, Hu X F, Zhang W J. Remaining useful life prediction based on health index similarity. *Reliability Engineering & System Safety*, 2019, 185: 502-510, <https://doi.org/10.1016/j.res.2019.02.002>.
18. Benkedjough T, Medjaher K, Zerhouni N, et al. Health assessment and life prediction of cutting tools based on support vector regression, *Journal of Intelligent Manufacturing*, 2015, 26: 213-223, <https://doi.org/10.1007/s10845-013-0774-6>.
19. Liu D, Duan X C, Wang S P, et al. A reliability estimation method based on signal feature extraction and artificial neural network supported Wiener process with random effects, *Applied Soft Computing*, 2023, 136: 110044, <https://doi.org/10.1016/j.asoc.2023.110044>.
20. Aye S, Heyns P. An integrated Gaussian process regression for prediction of remaining useful life of slow speed bearings based on acoustic emission, *Mechanical Systems and Signal Processing*, 2017, 84: 485-498, <https://doi.org/10.1016/j.ymssp.2016.07.039>.
21. Song C Y, Liu K B. Statistical degradation modeling and prognostics of multiple sensor signals via data fusion: A composite health index approach, *IIEE Transactions*, 2018, 50(10): 853-867, <https://doi.org/10.1080/24725854.2018.1440673>.
22. Li Z, Wu J, Yue X. A shape-constrained neural data fusion network for health index construction and residual life prediction, *IEEE Transactions on Neural Networks and Learning Systems*, 2020, 32(11): 5022-5033, <https://doi.org/10.1109/TNNLS.2020.3026644>.
23. Li N P, Gebrael N, Lei Y G, et al. Remaining useful life prediction based on a multi-sensor data fusion model, *Reliability Engineering & System Safety*, 2021, 208: 107249, <https://doi.org/10.1016/j.res.2020.107249>.
24. Wu B, Zeng J, Shi H, et al. Multi-sensor information fusion-based prediction of remaining useful life of nonlinear Wiener process, *Measurement Science and Technology*, 2022, 33(10): 105106, <https://doi.org/10.1088/1361-6501/ac7636>.

25. Chen Z, Xia T B, Zhou D, et al. A health index construction framework for prognostics based on feature fusion and constrained optimization. *IEEE Transactions on Instrumentation and Measurement*, 2021, 70: 1-15, [https://doi: 10.1109/TIM.2021.3104414](https://doi.org/10.1109/TIM.2021.3104414).
26. Liu M J, Dong Z S, Shi H. Multi-Sensor Information Fusion and Multi-Model Fusion-Based Remaining Useful Life Prediction of Fan Slewing Bearings with the Nonlinear Wiener Process, *Sustainability*, 2023, 15(15): 12010, <https://doi.org/10.3390/su151512010>.
27. Wang F T, Liu X T, Deng G, et al. Remaining life prediction method for rolling bearing based on the long short-term memory network, *Neural processing letters*, 2019, 50: 2437-2454, <https://doi.org/10.1007/s11063-019-10016-w>.
28. Zhang B, Zhang L J, Xu J W. Degradation feature selection for remaining useful life prediction of rolling element bearings, *Quality and Reliability Engineering International*, 2016, 32(2): 547-554, <https://doi.org/10.1002/qre.1771>.
29. Liao L X. Discovering prognostic features using genetic programming in remaining useful life prediction, *IEEE Transactions on Industrial Electronics*, 2013, 61(5): 2464-2472, <https://doi.org/10.1109/TIE.2013.2270212>.
30. Pan Y P, Er M J, Li X, et al. Machine health condition prediction via online dynamic fuzzy neural networks, *Engineering Applications of Artificial Intelligence*, 2014, 35: 105-113, <https://doi.org/10.1016/j.engappai.2014.05.015>.
31. Guo L, Li N P, Jia F, et al. A recurrent neural network based health indicator for remaining useful life prediction of bearings, *Neurocomputing*, 2017, 240: 98-109, <https://doi.org/10.1016/j.neucom.2017.02.045>.
32. Chen D, Qin Y, Wang Y, Zhou J. Health indicator construction by quadratic function-based deep convolutional auto-encoder and its application into bearing RUL prediction. *ISA transactions*, 2021, 114: 44-56, <https://doi.org/10.1016/j.isatra.2020.12.052>.
33. Shakya P, Kulkarni M S, Darpe A K. A novel methodology for online detection of bearing health status for naturally progressing defect, *Journal of Sound and Vibration*, 2014, 333(21): 5614-5629, <https://doi.org/10.1016/j.jsv.2014.04.058>.
34. Guan Q L, Wei X K, Bai W F, et al. Two-stage degradation modeling for remaining useful life prediction based on the Wiener process with measurement errors, *Quality and Reliability Engineering International*, 2022, 38(7): 3485-3512, <https://doi.org/10.1002/qre.3147>.
35. Lee M, Whitmore G A. Threshold regression for survival analysis: modeling event times by a stochastic process reaching a boundary, *Statistical Science*, 2006, 21(4): 501-513, <https://doi.org/10.1214/088342306000000330>.
36. Rauch H E, Tung F, Striebel C T. Maximum likelihood estimates of linear dynamic systems. *AIAA Journal*. 1965, 3, 1445-1450, <https://doi.org/10.2514/3.3166>.
37. Wang B, Lei Y G, Li N P, et al. A hybrid prognostics approach for estimating remaining useful life of rolling element bearings, *IEEE Transactions on Reliability*, 2018, 69(1): 401-412, <https://doi.org/10.1109/TR.2018.2882682>.
38. Si X S, Wang W, Hu C H, et al. A Wiener-process-based degradation model with a recursive filter algorithm for RUL estimation, *Mechanical Systems and Signal Processing*, 2013, 35(1-2): 219-237, <https://doi.org/10.1016/j.ymssp.2012.08.016>.